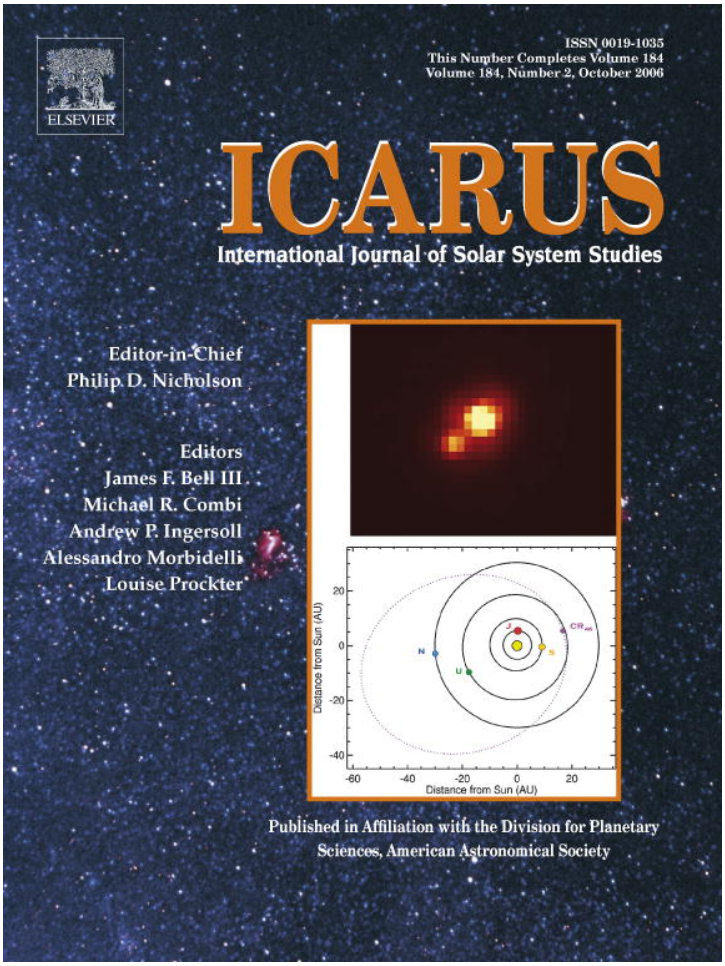

Available online at www.sciencedirect.com
ScienceDirect
Icarus 184 (2006) 589–601
ICARUS
www.elsevier.com/locate/icarus

A distant planetary-mass solar companion may have produced distant detached objects

Rodney S. Gomes [a], John J. Matese [b,*], Jack J. Lissauer [c]

[a] *Observatório Nacional, Rua General José Cristino, 77, 20921-400 Rio de Janeiro, RJ, Brazil*
[b] *Department of Physics, University of Louisiana at Lafayette, Lafayette, LA 70504-4210, USA*
[c] *Space Science and Astrobiology Division, MS 245-3, NASA Ames Research Center, Moffett Field, CA 94035, USA*

Received 16 December 2005; revised 18 May 2006

Available online 26 July 2006

Abstract

Most known trans-neptunian objects (TNO's) are either on low eccentricity orbits or could have been perturbed to their current trajectories via gravitational interactions with known bodies. However, one or two recently-discovered TNO's are distant detached objects (DDO's) (perihelion, $q > 40$ AU and semimajor axis, $a > 50$ AU) whose origins are not as easily understood. We investigate the parameter space of a hypothetical distant planetary-mass solar companion which could detach the perihelion of a Neptune-dominated TNO into a DDO orbit. Perturbations of the giant planets are also included. The problem is analyzed using two models. In the first model, we start with a distribution of undetached, low-inclination TNO's having a wide range of semimajor axes. The planetary perturbations and the companion perturbation are treated in the adiabatic, secularly averaged tidal approximation. This provides a starting point for a more detailed analysis by providing insights as to the companion parameter space likely to create DDO's. The second model includes the companion and the planets and numerically integrates perturbations on a sampling that is based on the real population of scattered disk objects (SDO's). A single calculation is performed including the mutual interactions and migration of the planets. By comparing these models, we distinguish the distant detached population that can be attributable to the secular interaction from those that require additional planetary perturbations. We find that a DDO can be produced by a hypothetical Neptune-mass companion having semiminor axis, $b_c \leqslant 2000$ AU or a Jupiter-mass companion with $b_c \leqslant 5000$ AU. DDO's produced by such a companion are likely to have small inclinations to the ecliptic only if the companion's orbit is significantly inclined. We also discuss the possibility that the tilt of the planets' invariable plane relative to the solar equatorial plane has been produced by such a hypothetical distant planetary-mass companion. Perturbations of a companion on Oort cloud comets are also considered.

Keywords: Trans-neptunian belt; Comets, dynamics

1. Introduction

Nearly 1000 minor planets orbiting the Sun on paths that are primarily or entirely beyond the orbit of Neptune have received official designations from the Minor Planet Center. Almost all of these trans-neptunian objects (TNO's) either have low eccentricity orbits with semimajor axes $a < 50$ AU, are trapped in mean-motion orbital resonances with Neptune, or travel on orbits that at least at times drop down close enough to Neptune to have their dynamics controlled by gravitational interactions with Neptune or other giant planets. In contrast, two objects, 2000 CR_{105} ($q = 44$ AU, $a = 221$ AU, $i = 22.7°$; discovered in the Deep Ecliptic Survey) and 90377 Sedna (2003 VB_{12}; $q = 76$ AU, $a = 489$ AU, $i = 11.9°$; Brown et al., 2004), travel on eccentric orbits with sufficiently distant (detached) perihelia that they cannot have been perturbed onto their current trajectories by the actions of the planets as currently configured (Emel'yanenko et al., 2003). Similarly, the aphelia of Sedna and 2000 CR_{105} are too small for the galactic tides to have detached them from the influence of the known planets. In this sense, they appear to be the first discovered true inner Oort cloud objects.

Gomes et al. (2005a) discuss resonant mechanisms for converting objects in the scattered disk (SD, defined as having

* Corresponding author. Fax: +1 337 482 6699.
E-mail address: matese@louisiana.edu (J.J. Matese).

0019-1035/$ – see front matter
doi:10.1016/j.icarus.2006.05.026

semimajor axis exceeding 50 AU) into distant detached objects (DDO's). They find that resonance capture during the epoch of giant planet migration can produce DDO's such as 2000 CR_{105}, but the processes that they simulated cannot produce DDO's with $a > 260$ AU. Moreover, Sedna's inclination is too low for its orbit to be produced by the combination of a mean motion resonance and the Kozai mechanism with Neptune. Morbidelli and Levison (2004) consider, and reject, three additional mechanisms, (i) the passage of Neptune through a high-eccentricity stage, (ii) the past existence of massive planetary embryos in the Kuiper belt or scattered disk, and (iii) tidal perturbations on scattered disk objects exerted by a hypothetical massive transneptunian disk at early epochs. The only options which they find to give satisfactory results are the passage of a low-velocity solar-mass star at about 800 AU, or the capture of extrasolar planetesimals from a low-mass star or brown dwarf encountering the Sun at low velocity. Such close, slow encounters are only plausible when the Sun was young and surrounded by siblings born from the same molecular cloud. Morbidelli and Levison (2004) note that creating a population of "extended scattered disk objects" in which the largest orbits also have the largest perihelia requires a perturbation "from the outside," but they do not discuss the possibility that the external perturbation could come from a distant planetary-mass solar companion. We consider that option here.

Our goal is to delineate the possible parameter space of a hypothetical solar companion which would be capable of detaching the orbit of an SDO from the dominance of Neptune. Section 2 describes an investigation of this problem using the adiabatic secular analysis and presents the ranges of companion parameters that could produce a Sedna-like DDO in this approximation. Direct numerical integrations including the four major planets and the hypothetical solar companion are then presented in Section 3. In Section 4, we discuss the possibility that a companion has produced the observed misalignment between the invariable plane and the Sun's equatorial plane and also consider the effects that a companion would have on Oort cloud comets. We compare the results for secular and full perturbations, summarize and give our conclusions in Section 5.

2. Perturbing scattered disk objects: the secular analysis

The equations of motion of the eccentricity vector and the angular momentum vector (see Fig. 1) of an SDO have been analyzed by Matese et al. (2006). The tidal perturbations of a hypothetical distant planetary-mass solar companion (M_c, r_c), and the known planets (M_p, r_p), treated as massive rings, are included in a secularly averaged manner, with possible resonances and impulsive interactions being ignored. The inferences discussed in this section should be used only as a guide for a more detailed analysis, contained in the next section, in which these effects are not ignored.

We approximate the companion motion as an invariant ellipse of mass and orbital parameters M_c, a_c, e_c, i_c having orbit normal $\hat{\mathbf{n}}_c$. The heliocentric SDO position is denoted by $\mathbf{r}$; the scaled angular momentum vector, $\mathbf{h}$, and the eccentricity vector, $\mathbf{e}$, are given by

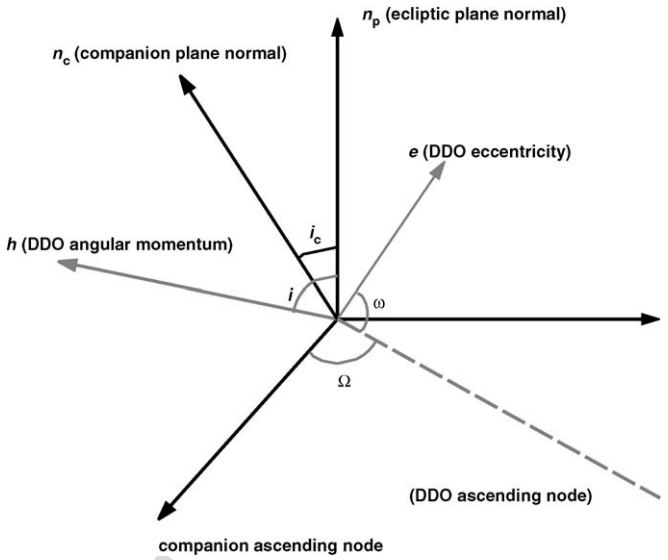

Fig. 1. Orientation definitions of the orbital vectors of the hypothetical planetary-mass companion and the distant detached object.

$$\mathbf{h} \equiv \frac{\mathbf{r}\times\dot{\mathbf{r}}}{\sqrt{\mu a}}, \qquad \mathbf{e} \equiv \frac{\dot{\mathbf{r}}\times\mathbf{h}}{\sqrt{\mu/a}} - \hat{\mathbf{r}}, \tag{1}$$

where $\mu \equiv GM \equiv G(M_\odot + \sum_p M_p)$ includes the contributions from the known planets as well as the Sun. Sequentially performing secular averages over the short (SDO) orbital period and the long (companion) orbital period, in the tidal limits we obtain

$$\langle\dot{\mathbf{h}}\rangle = \frac{2(\hat{\mathbf{n}}_p\cdot\mathbf{h})\hat{\mathbf{n}}_p\times\mathbf{h}}{h^5\tau_p} + \frac{5(\hat{\mathbf{n}}_c\cdot\mathbf{e})\hat{\mathbf{n}}_c\times\mathbf{e} - (\hat{\mathbf{n}}_c\cdot\mathbf{h})\hat{\mathbf{n}}_c\times\mathbf{h}}{\tau_c}, \tag{2}$$

$$\langle\dot{\mathbf{e}}\rangle = \frac{(h^2 - 3(\hat{\mathbf{n}}_p\cdot\mathbf{h})^2)\mathbf{h}\times\mathbf{e} - 2(\hat{\mathbf{n}}_p\cdot\mathbf{h})(\hat{\mathbf{n}}_p\cdot(\mathbf{h}\times\mathbf{e}))\mathbf{h}}{h^7\tau_p} + \frac{\mathbf{h}\times\mathbf{e} + 4(\hat{\mathbf{n}}_c\cdot\mathbf{e})\hat{\mathbf{n}}_c\times\mathbf{h} + (\hat{\mathbf{n}}_c\cdot(\mathbf{h}\times\mathbf{e}))\hat{\mathbf{n}}_c}{\tau_c}, \tag{3}$$

where $\hat{\mathbf{n}}_p$ is the normal direction to the ecliptic plane with

$$\frac{1}{\tau_p} \equiv \frac{3\sum_p \mu_p r_p^2}{8\sqrt{\mu a^7}} \quad \text{and} \quad \frac{1}{\tau_c} \equiv \frac{3M_c\sqrt{\mu a^3}}{4Mb_c^3}, \tag{4}$$

where $b_c \equiv a_c\sqrt{1-e_c^2}$ is the semiminor axis of the companion. These analytic forms are obtained using *Mathematica* (Wolfram Research, 2003). The largest planetary perturbation is from Neptune, which contributes 41% to the total.

We see that the secular planetary interaction produces orbit normal precession around $\hat{\mathbf{n}}_p$, while a similar term in the secular companion interaction produces orbit normal precession around $\hat{\mathbf{n}}_c$. It is the term proportional to $(\hat{\mathbf{n}}_c\cdot\mathbf{e})\hat{\mathbf{n}}_c\times\mathbf{e}$ that serves to change q for large-eccentricity SDO's. Note that this term vanishes if the SDO and the companion are coplanar. The analysis reproduces the well-known result that in the secular approximation planetary perturbations alone do not change e (Goldreich, 1965). The secularly averaged equations depend on the companion elements through the quantities $\hat{\mathbf{n}}_c$ and τ_c. There are several symmetries evident in the equations, such as their

invariance when $\hat{\mathbf{n}}_c \to -\hat{\mathbf{n}}_c$, i.e., $i_c \to \pi - i_c$, and their independence of the companion perihelion direction, $\hat{\mathbf{e}}_c$.

Orienting the coordinate axes as shown in Fig. 1, we see that the companion can be characterized by two parameters, i_c and

$$\rho_c \equiv \frac{M_c}{b_c^3}, \tag{5}$$

a strength parameter, both assumed to be constant here. The DDO orbit is characterized by a secularly constant semimajor axis, a, and four variable elements i, ω, Ω and e. The six coupled equations for the components of $\mathbf{e}$ and $\mathbf{h}$ are restricted by the two conserved quantities, $\mathbf{h} \cdot \mathbf{e} = 0$ and $h^2 + e^2 = 1$, which serve as checks on our numerical solutions.

Our goal here is to guide the numerical modeling described in the next section, and as such the analysis is not meant to provide meaningful detailed predictions of the actual distributions. In that context, we assume that each possible SDO progenitor orbit of an DDO object was dominated by Neptune with initial values $q_\circ = 32 \leftrightarrow 38$ AU, $i_\circ = 0 \leftrightarrow 15°$. These initial values are randomly sampled in the indicated ranges, with a randomly chosen between $q_\circ$ and 1000 AU. The remaining two initial elements of the token orbits, $\Omega_\circ$, $\omega_\circ$, are randomly sampled over their ranges $0 \leftrightarrow 360°$. We then integrate the equations over an interval of 2×10^9 years and record a, q and i at that time. The distributions are essentially unchanged if integration times are extended beyond 2×10^9 years.

In Fig. 2, we show the results for a single value of $\rho_c = 1.5 \times 10^{-14}$ $M_\odot$ AU^{-3}. For example, this would describe the perturbation of a Neptune-mass companion, $M_c = 5 \times 10^{-5}$ $M_\odot$, in an orbit with $b_c = 1500$ AU, or equivalently a jovian-mass companion, $M_c = 10^{-3}$ $M_\odot$, in an orbit with $b_c = 4000$ AU. We see that the ability of the secular companion perturbation to detach the perihelion of an SDO is significantly reduced when a is small. It also shows that the DDO maintains the modest (initial) inclinations of the SDO only if the companion is itself significantly inclined to the ecliptic.

The general features of Fig. 2 hold for other values of ρ_c with a single exception, the value of a for which the onset of detachment occurs. We can estimate this critical value as follows. In Eq. (2), we compare the timescale for planetary-induced precession with that of the companion perturbation term causing detachment. Ignoring the angular factors, for near-parabolic SDO's the ratio is strongly dependent on a:

$$\frac{5e^2/\tau_c}{2/(h^3\tau_p)} \quad \longrightarrow \quad 10\sqrt{2}\rho_c \frac{q^{3/2}a^{7/2}}{\sum_p M_p r_p^2}. \tag{6}$$

Detachment occurs when this ratio is $\geqslant O(1)$. Inserting planetary parameters and an initial value of $q_\circ \approx 35$ AU and setting the ratio equal to 1 yields an estimate of the value of a for which the onset of detachment occurs, $a_{\rm detach} \approx 490$ AU for the parameters used in Fig. 2. This is in reasonable agreement with the numerical results presented in Fig. 2. More generally, the estimate is

$$a_{\rm detach} \approx 550 \text{ AU } \left(\rho_c/10^{-14} \text{ M}_\odot \text{ AU}^{-3}\right)^{-2/7} \tag{7}$$

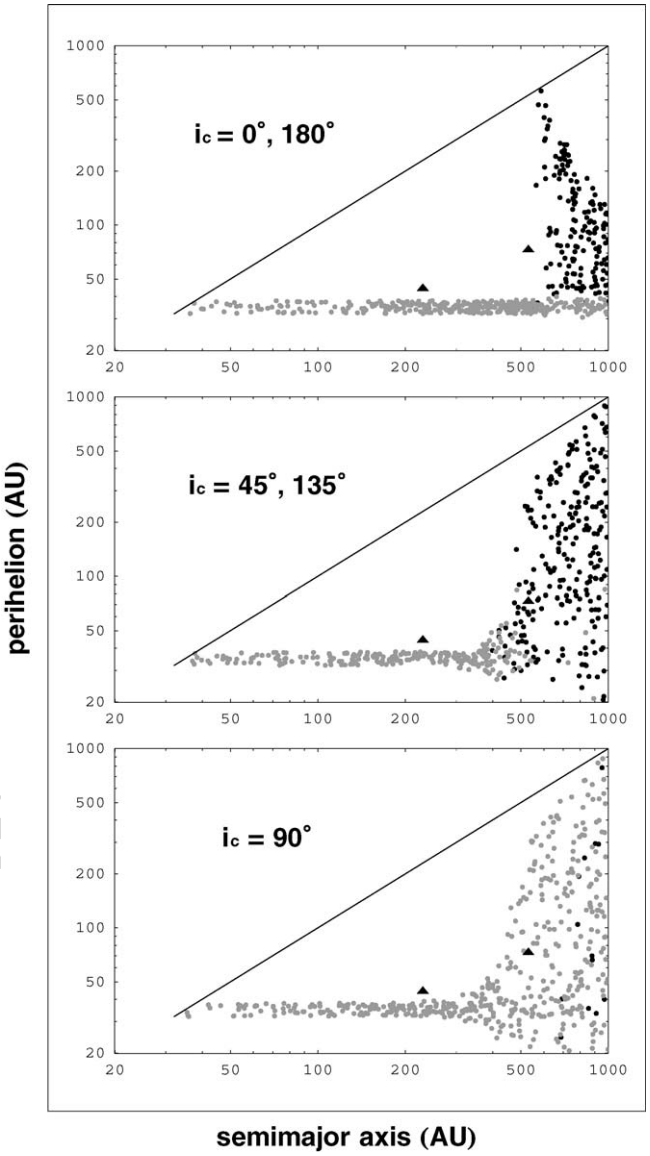

Fig. 2. The effects of secular perturbations, integrated over 2×10^9 years, of scattered disk objects for the companion strength parameter $\rho_c \equiv M_c/b_c^3 = 1.5 \times 10^{-14}$ $M_\odot$ AU^{-3} and various companion inclinations i_c. The SDO's have perihelia between 32 and 38 AU at the beginning of the integrations. Equivalent example parameter sets are $b_c \equiv a_c\sqrt{1-e_c^2} = 1500$ AU, $M_c = 5 \times 10^{-5}$ $M_\odot$ and $b_c = 3000$ AU, $M_c = 4 \times 10^{-4}$ $M_\odot$. Gray dots $\leftrightarrow i < 15°$, black dots $\leftrightarrow i > 15°$, triangles $\leftrightarrow$ Sedna and 2000 CR$_{105}$.

in the secular approximation. Specifically, we find that detaching to perihelia >75 AU at Sedna's semimajor axis requires

$$M_c > 0.8 \times 10^{-14} \text{ M}_\odot \text{ AU}^{-3} b_c^3. \tag{8}$$

A distant companion orbit is subject to perturbations from passing stars and the galactic tide. Therefore, these parameters essentially describe the epoch when companion interactions with DDO's are strongest, i.e., when ρ_c is largest. The galactic tide affects e_c and i_c, but changes are small for $a_c < 10{,}000$ AU. In 4.5×10^9 years osculations proceed through approximately one half-cycle when $a_c \approx 20{,}000$ AU.

To illustrate the subtle interplay between secular and impulsive interactions, we show in Fig. 3 an example case of

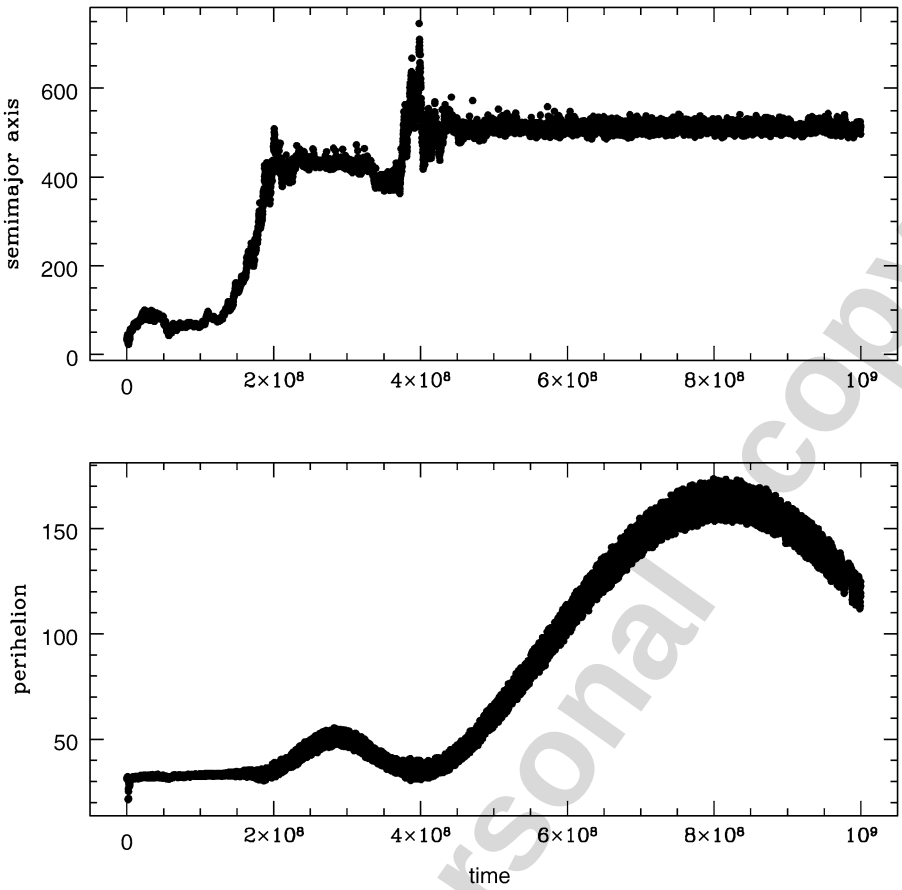

Fig. 3. An example of the orbital evolution of a single massless particle interacting with the four known giant planets and the companion, obtained by direct numerical integration. The particle is initially in a near-circular small-inclination orbit just beyond Neptune and the companion has parameters $a_c = 1500$ AU, $e_c = 0$, $i_c = 90°$, $M_c = 5 \times 10^{-5}$ $M_\odot$ and $\rho_c = 1.5 \times 10^{-14}$ $M_\odot$ AU^{-3}.

the orbital evolution of a single massless particle interacting with the four known giant planets and the companion, obtained by direct numerical integration as discussed in Section 3.1. The particle is initially in a near-circular small-inclination orbit just beyond Neptune, and the companion has parameters $a_c = 1500$ AU, $e_c = 0$, $i_c = 90°$, $M_c = 5 \times 10^{-5}$ $M_\odot$ and $\rho_c = M_c/b_c^3 = 1.5 \times 10^{-14}$ $M_\odot$ AU^{-3}. During the initial stages of the 10^9 year integration, impulses by Neptune slowly pump the semimajor axis to ≈450 AU at which time companion secular effects are strong enough to detach it from Neptune dominance. Detachment occurs at a value of a that is in reasonable agreement with the analytic estimate for $a_{\rm detach}$ given in Eq. (7). The secular interaction can return the particle to Neptune dominance, as shown by Matese et al. (2006). This leads to a second brief impulsively dominated epoch and eventually the particle is secularly detached for a second time when $a \approx 500$ AU. These impulsive effects are ignored in the secular analysis illustrated in Fig. 2 and therefore a secular approximation cannot produce a complete description of distributions.

We can qualitatively understand the competing processes by considering the a-dependence of the energy-pumping and perihelion migration timescales during the impulsively dominated epoch

$$\frac{{\rm d}a^{-1}}{{\rm d}t} \propto a^{-3/2} \quad \text{and} \quad \frac{{\rm d}q}{{\rm d}t} \propto \frac{ah}{\tau_c} \propto a^2. \tag{9}$$

The illustration shown in Fig. 3 indicates that when $a \approx 400$ AU, q can grow sufficiently rapidly that energy pumping effectively ceases, i.e., detachment occurs. Both detachment and re-attachment occur when $q \approx 40$ AU.

3. Perturbing scattered disk objects: direct numerical integrations

Two models have been used for direct numerical integrations. The first model considers all four major planets (at their present orbits) and the companion as perturbers. The particles are massless and are started near Neptune so as to get promptly scattered. There are initially 1000 particles; 500 particles are started uniformly with a from 27 to 29 AU; 500 particles are started uniformly with a from 31 to 33 AU. The initial eccentricities are randomly distributed between 0 and 0.1 and the initial inclinations randomly distributed between 0 and 1°.

The second model includes the four planets started in compact orbits and a disk of massive particles just outside the outermost planet; only a single run was performed for this computationally-demanding model. The particles perturb the planets and companion and these perturb all objects, but the particles do not affect one another. This model induces a planetary migration in an abrupt sense as described in Gomes et al. (2005b), Tsiganis et al. (2005) and Morbidelli et al. (2005)

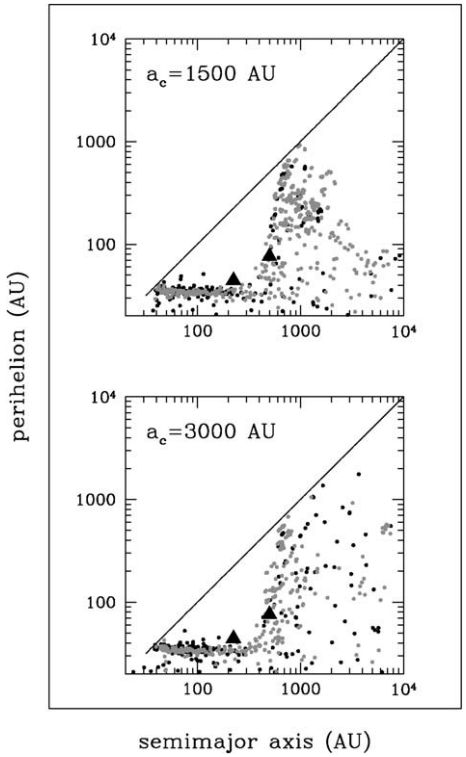

Fig. 4. Direct numerical integration were undertaken with all major planets and a companion with $\rho_c = 1.5 \times 10^{-14}$ $M_\odot$ AU^{-3} as perturbers. Distributions of semimajor axes and perihelia of particles started near Neptune after 10^9 years of evolution are plotted. Upper panel $\leftrightarrow$ $M_c = 5 \times 10^{-5}$ $M_\odot$, $a_c = 1500$ AU, $e_c = 0$, $i_c = 90°$; lower panel $\leftrightarrow$ $M_c = 4 \times 10^{-4}$ $M_\odot$, $a_c = 3000$ AU, $e_c = 0$, $i_c = 90°$. Gray dots $\leftrightarrow$ $i < 15°$, black dots $\leftrightarrow$ $i > 15°$, triangles $\leftrightarrow$ Sedna and 2000 CR_{105}. These plots can be compared to the secular analysis results given in the bottom panel of Fig. 2.

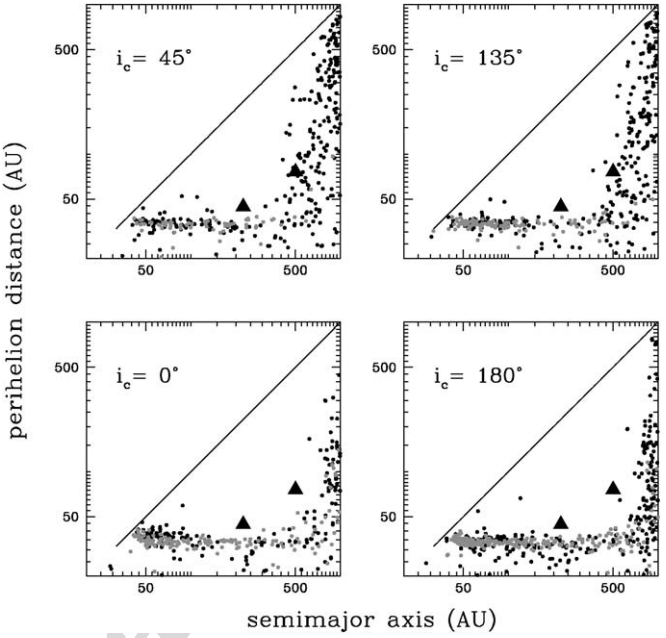

Fig. 5. At 10^9 years, the distributions of semimajor axes and perihelia of particles started near Neptune. Direct numerical integration were undertaken with all major planets and a companion with $\rho_c = 1.5 \times 10^{-14}$ $M_\odot$ AU^{-3} as perturbers. Companion parameters $\leftrightarrow$ $M_c = 5 \times 10^{-5}$ $M_\odot$, $a_c = 1500$ AU, $e_c = 0$; inclinations as indicated in each panel. Gray dots $\leftrightarrow$ $i < 15°$, black dots $\leftrightarrow$ $i > 15°$, triangles $\leftrightarrow$ Sedna and 2000 CR_{105}. These plots can be compared to the secular analysis results given in Fig. 2.

pointing towards an explanation of the lunar heavy bombardment, the origin of the Trojans and the present orbital structure of the giant planets. We also considered the galactic tide in this run.

The set of runs for the first model used 1 year for the steplength. For the migration model 0.5 year was used in the beginning and 1 year after the LHB had calmed down and the planets were close to their present orbits. All integrations were performed using the MERCURY package (Chambers, 1999).

3.1. Four known planets and companion

For this model (massless particles), we begin by showing examples meant to compare with the semianalytical approach of Section 2. First we compare the distribution created by two different companions. Both components have circular orbits and their semimajor axes and masses are, respectively, $a_c = 1500$ AU, $M_c = 5 \times 10^{-5}$ $M_\odot$ and $a_c = 3000$ AU, $M_c = 4 \times 10^{-4}$ $M_\odot$. These two sets of companion's parameters correspond to the same strength parameter, ρ_c [Eq. (5)], and should induce the same a–q distribution for a common companion inclination if the secular approximation is appropriate. Each numerical integration simulated 10^9 years. Fig. 4 shows the pair of distributions for $i_c = 90°$. The inner border of the detached regions and the distributions of low inclination objects are quite similar, suggesting that the secular effects as developed in Section 2 play a prominent role in the establishment of the a–q distribution of detached scattered objects. Differences with the direct numerical integration model are of two kinds. First, the larger, more distant companion is more effective at detaching perihelia of scattered objects with larger semimajor axes. Second, the smaller, closer companion forms a 28% more massive inner Oort cloud at 10^9 years. The reason for this deserves a deeper investigation. A larger M_c raises the perihelia of scattered objects in a shorter timescale, but also brings them back to Neptune-crossing orbits in the same short timescale. Moreover, the companion can directly scatter the objects away from the inner Oort cloud. There must be an ideal companion (mass, distance from the Sun, eccentricity and inclination) that will create the largest inner Oort cloud population at the Solar System's age, but this goes beyond the scope of this paper. Note also that even for this high value of i_c there is no significant Kozai mechanism altering the companion's orbit; e_c only goes up to 0.05 and i_c varies by only $\pm 2°$.

For the smaller, closer, companion, integrations with $i_c = 0°$, 45°, 135°, 180° were also undertaken. The a–q distributions created by this companion are shown in Fig. 5. The inclinations equidistant from 90° are placed side by side so as to compare their similarities. In principle, by the secular theory these distributions should be equivalent, which is fairly well confirmed by comparing Figs. 4 and 5 with Fig. 2.

We conclude that secular analysis fails where it is expected to fail, i.e., when the tidal approximation is invalid, particularly when impulses can occur. Nonetheless, it provides a useful

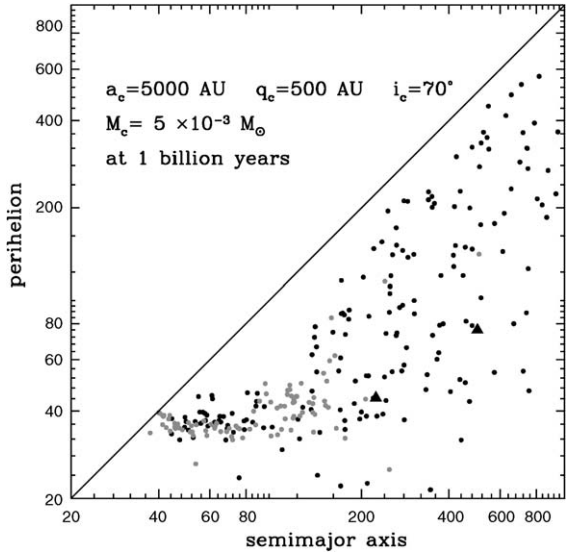

Fig. 6. Distributions of semimajor axes and perihelia of particles started near Neptune. Direct numerical integration were undertaken with all major planets and a companion with $\rho_c = 4.8 \times 10^{-13}$ $M_\odot$ AU^{-3} and $i_c = 70°$ as perturbers. Companion parameters $\leftrightarrow M_c = 5 \times 10^{-3}$ $M_\odot$, $a_c = 5000$ AU, $e_c = 0.9$. Gray dots $\leftrightarrow i < 15°$, black dots $\leftrightarrow i > 15°$, triangles $\leftrightarrow$ Sedna and 2000 CR_{105}.

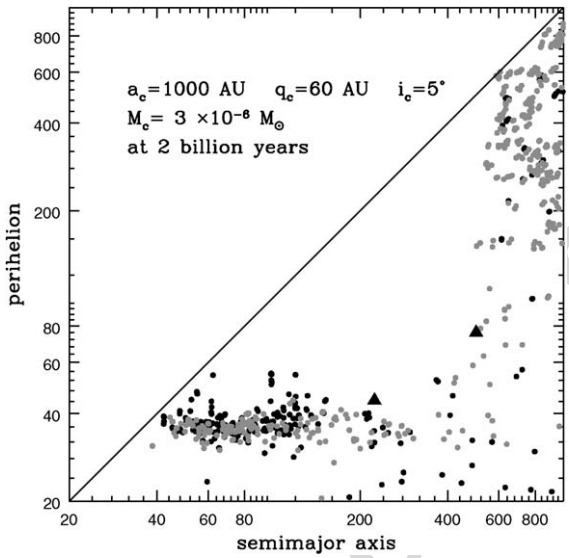

Fig. 7. Same as Fig. 6, except that the companion parameters $\leftrightarrow M_c = 3 \times 10^{-6}$ $M_\odot$, $a_c = 1000$ AU, $e_c = 0.94$, $i_c = 5°$, and thus $\rho_c = 7.6 \times 10^{-13}$ $M_\odot$ AU^{-3}.

approach to delineating the parameter space that needs to be numerically studied in investigating the possibility that the distant detached population (DDP) was produced by a hypothetical distant planetary mass companion.

Now we give three other examples covering a wide range of masses and semimajor axes for the companion. High eccentricities are used in these cases. In one extreme, we consider a companion with $a_c = 5000$ AU, $e_c = 0.9$, $i_c = 70°$ and $M_c = 5 \times 10^{-3}$ $M_\odot$. Fig. 6 shows the a–q distribution at 1 billion years of integration. This companion has a $\rho_c = 4.8 \times 10^{-13}$ $M_\odot$ AU^{-3}, thus much higher than those given in the examples above and also higher than the value needed to detach Sedna and 2000 CR_{105} [see Eq. (7)]. In fact, Fig. 6 shows that DDO's are produced not only at Sedna's semimajor axis but also at 2000 CR_{105} semimajor axis. DDO's are indeed produced for semimajor axes just above 100 AU. This example is instructive as these parameters for the companion also induce a 6° tilt of the invariable plane at the age of the Solar System (see Section 4.1).

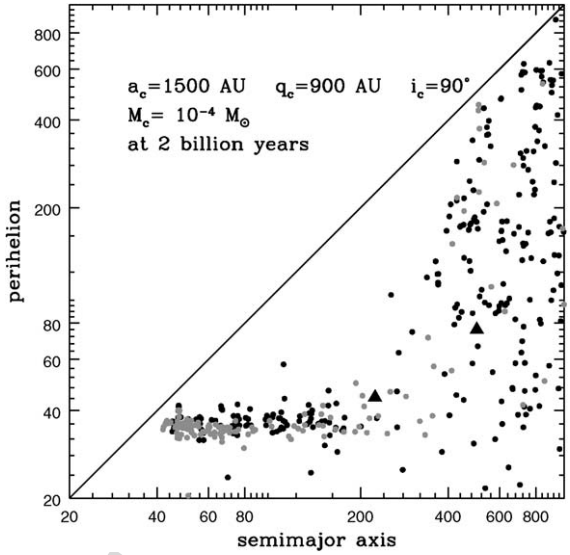

Fig. 8. Same as Figs. 6 and 7, except for a companion parameters $\leftrightarrow M_c = 10^{-4}$ $M_\odot$, $a_c = 1500$ AU, $e_c = 0.4$, $i_c = 90°$, and thus $\rho_c = 3.8 \times 10^{-14}$ $M_\odot$ AU^{-3}.

The second case examines another extreme with an Earth mass planet ($M_c = 3 \times 10^{-6}$ $M_\odot$), $a_c = 1000$ AU, $e_c = 0.94$, $i_c = 5°$, that corresponds to $\rho_c = 7.6 \times 10^{-14}$ $M_\odot$ AU^{-3}, again large enough to detach Sedna but not 2000 CR_{105}. Fig. 7 shows the a–q distribution induced by this planet at 2 billion years of integration. Sedna is inside the IOC created by this Earth mass planet, but a 2000 CR_{105} orbit is hardly detached by this planet. In this case the secular theory is inappropriate since the companion orbit is partially interior to DDO orbits. Secular theory fails in that it predicts that detached orbits should have large inclinations, the opposite of that obtained in the numerical analysis.

The third eccentric example is for a companion with $a_c = 1500$ AU, $e_c = 0.4$, $i_c = 90°$ and $M_c = 10^{-4}$ $M_\odot$. These parameters correspond to a $\rho_c = 3.8 \times 10^{-14}$ $M_\odot$ AU^{-3}, which is large enough to detach Sedna but not 2000 CR_{105} according to Eq. (7). The a–q distribution at 2 billion years of integration is shown in Fig. 8. We see Sedna well inside an IOC whose members have semimajor axes as low as ∼200 AU. This also includes 2000 CR_{105}, a more optimistic result than predicted by the secular theory. As Fig. 5 suggests, 90° companions create IOC's that extend to lower semimajor axes.

3.2. Four migrating planets, companion and galactic tide

One single integration was done with a fairly complete evolutionary model. Here we suppose that the giant planets had primordially more compact orbits and there was a disk of plan-

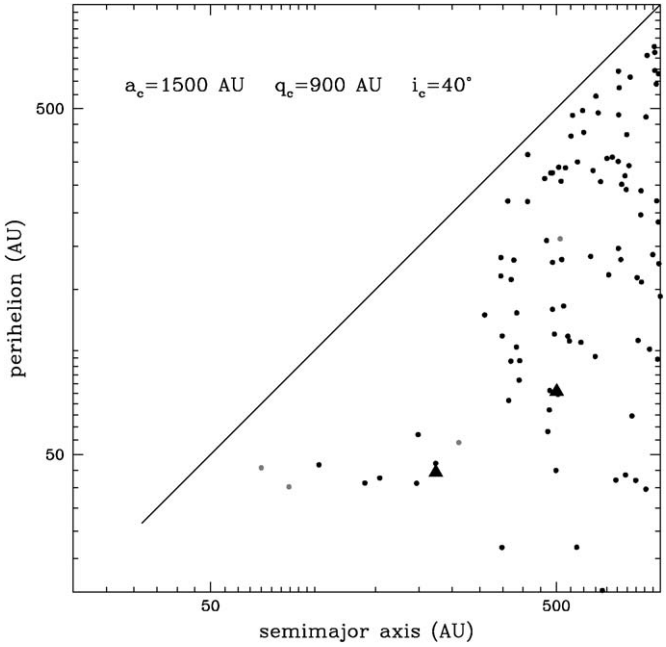

Fig. 9. Distributions of semimajor axes and perihelia of particles started in a disk just outside the giant planets in initial compact orbits. Direct numerical integrations are done with the major planets and a companion as perturbers. The particles have mass and perturb the planets and companion (but not one another), inducing planetary migration. The galactic tide was also included in this integration. The results are after 4.5×10^9 years, when the planets are near their present position. Companion parameters $\leftrightarrow M_c = 10^{-4}$ $M_\odot$, $a_c = 1500$ AU, $e_c = 0.4$, $\rho_c = 3.8 \times 10^{-14}$ $M_\odot$ AU^{-3}. Gray dots $\leftrightarrow i < 15°$, black dots $\leftrightarrow i > 15°$, triangles $\leftrightarrow$ Sedna and 2000 CR_{105}.

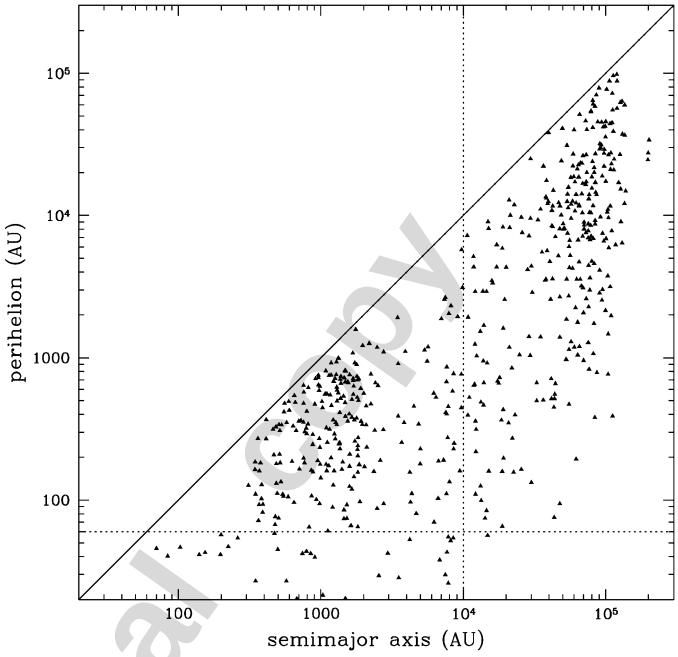

Fig. 10. Same as Fig. 9 in a larger scale that also shows particles trapped in the outer Oort cloud. Vertical and horizontal lines define each population, according to: inner Oort cloud $\leftrightarrow a < 10{,}000$ AU, $q > 60$ AU outer Oort cloud $\leftrightarrow a > 10{,}000$ AU, $q > 60$ AU scattered population $\leftrightarrow q < 60$ AU.

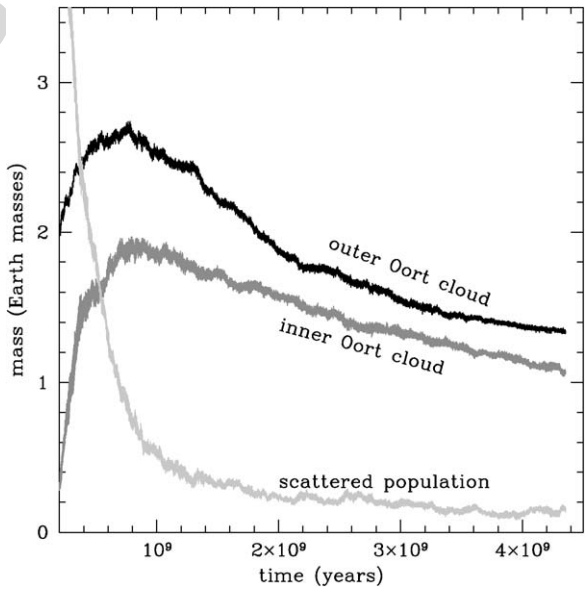

Fig. 11. Evolution of total mass trapped in the inner Oort cloud, outer Oort cloud and scattered populations, according to the same definitions used for Fig. 10.

etesimals just outside the outermost planet. The initial semimajor axes for the planets are 5.45, 8.18, 11.5 and 14.2 AU. The disk extends from 15.5 to 34 AU with a surface density proportional to r^{-1}. It is composed of 10,000 equally massive particles totaling 35 $M_\oplus$. Both the planets' and the particles' initial eccentricities and inclinations are small. A solar companion with parameters $a_c = 1500$ AU, $e_c = 0.4$, $i_c = 40°$ and $M_c = 10^{-4}$ $M_\odot$ (as in the final example presented in Section 3.1) as well as the galactic tidal perturbation are also included from the beginning of the integration. We used the same model for the galactic tide as that in Dones et al. (2005) and references therein. In this model, the accelerations in the directions defined by the galactic frame $\{\tilde{x}, \tilde{y}, \tilde{z}\}$ are:

$$F_{\tilde{x}} = \Omega_0^2 \tilde{x}, \qquad F_{\tilde{y}} = -\Omega_0^2 \tilde{y}, \qquad F_{\tilde{z}} = -4\pi G \rho_0 \tilde{z}, \tag{10}$$

with $\Omega_0 = 26$ km/s/kpc and $\rho_0 = 0.1$ $M_\odot/pc^3$.

Planetary migration is induced by the massive disk of planetesimals, whose parameters are chosen so that the planets stop near their present positions after scattering the planetesimals inwards and outwards according to a late heavy bombardment scenario (Gomes et al., 2005b; Tsiganis et al., 2005; Morbidelli et al., 2005). Fig. 9 shows the planetesimals a–q distribution obtained at Solar System age. Both Sedna and 2000 CR_{105} are shown in the a–q distribution induced by the companion. This single example, with $\rho_c = 4 \times 10^{-14}$ $M_\odot$ AU^{-3}, is instructive since it also estimates the total mass left in the inner Oort cloud. Fig. 10 presents the a–q distribution in another scale showing the distribution in the inner Oort cloud (induced by the companion), in the outer Oort cloud (modified by the galactic tide) and in the scattered population.

Fig. 11 shows the time evolution of the mass in each population. The limits for each population are defined as: inner Oort cloud: semimajor axis below 10,000 AU and perihelion above 60 AU; outer Oort cloud: semimajor axis above 10,000 AU; scattered population: semimajor axis below 10,000 AU and perihelion below 60 AU. With these definitions, we have at Solar System age: 1.07 $M_\oplus$ for the inner Oort cloud, 1.34 $M_\oplus$ for

the outer Oort cloud and 0.14 $M_\oplus$ for the scattered population. These numbers yield a ratio of the mass in the scattered population to the mass in the outer Oort cloud of 10%. In comparison with the total Oort cloud mass, this ratio drops to 6%. If we consider the more usual definition of the scattered population as $q < 45$ AU, then this ratio drops to 4%. These ratios are much higher than observational estimates, which yield a ratio of the scattered population mass to the Oort cloud mass no bigger than 0.5% (Dones et al., 2005; Duncan et al., 2004). The presence of a companion does not seem to change significantly these mass ratios as compared to simulations with no companion (Dones et al., 2005). On the other hand, cometary mass estimates from observations are based on the number of bodies in each population that succeeds in appearing as an observable comet, and the dynamics that rules the transfer of icy bodies in each cometary population to the observable zone also depends on the companion's perturbation. This should be taken into account to estimate the mass in each population based on observable comets. As an example, a scattered object with semimajor axis in the companion's influence zone may not follow its way from that disk to a JFC due to the companion's perturbation. For instance, it may have its perihelion increased once more. Before a deeper investigation on this issue is developed, one should not draw strong conclusions about the validity of the observed mass ratios in cometary populations in the presence of the perturbation from a solar companion. Fernández and Brunini (2000) consider various scenarios for a dense primordial environment of the Solar System. They find that a tightly bound inner Oort cloud containing ∼2 $M_\oplus$ can be formed at a timescale of a few million years. This is an amount of mass comparable to that shown in the complete Oort cloud in Fig. 11. The inclination distribution produced depends on the details of their modeling.

Assessing the consequences of these populations in the influx of comets into the inner Solar System requires additional simulations to obtain statistically robust results and thus are not investigated in this paper. However, it must be noted that the inner Oort cloud created by the companion model is 'live,' in contrast to the fossil populations created by passing star and dense early environment models. This means that the inner Oort cloud can continually replenish both the scattered population and the outer Oort cloud.

Fig. 12 shows the distribution of semimajor axes with perihelia for $q < 10$ AU, taken from the last 100 million years of the migration model. We notice an enhancement of low q objects for $a \sim 10{,}000$ AU and above, what is about expected from a single Oort cloud model, and an enhancement for $a < 2000$ AU, but for $q > 5$ AU. This figure seems to indicate that particles that attain small q by the companion's secular perturbation eventually get their semimajor axes decreased, thus feeding the Centaur population and eventually the Halley and Jupiter family comets populations. This point however needs a deeper investigation that our data are not able to confirm. This figure also suggests that the companion is not capable of sending a significant number of icy objects directly to the inner Solar System. Nonetheless, of all the particles whose q was detected lower than 10 AU during the last 100 million years of integration,

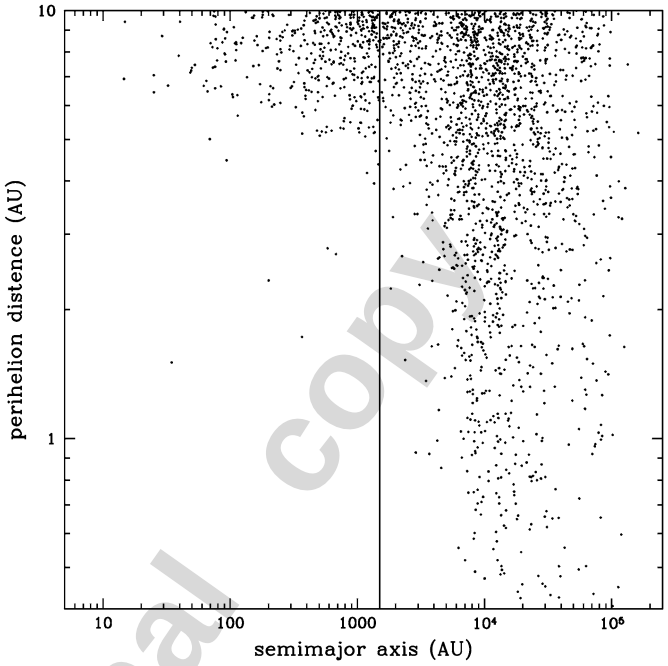

Fig. 12. Distributions of semimajor axis and perihelia coming from the last 100 million years of integration from the migration model, plotted for $q < 10$ AU. The vertical line indicates the companion's semimajor axis.

about 25% of them remained more than 5% of their time in the IOC created by this companion. This may indicate that the flux of comets from the OOC can be somewhat enhanced by the presence of this companion but not significantly.

It must also be noted that the 1.07 $M_\oplus$ mass estimated to inhabit the companion-induced inner Oort cloud is not too far from the estimate (however crude) by Brown et al. (2004) of 5 $M_\oplus$ for a population of Sedna-like objects. Note that this estimate should be revised downwards by roughly a factor of two because no Sedna-like bodies have been announced during the past two years despite continuing searches. The passing star model produces an inner Oort cloud that is an order of magnitude less massive.

3.3. A deeper focus at Sedna and 2000 CR_{105} orbits

In this section, we try to answer the question: "how good is an orbital distribution of objects created by a companion at explaining the orbits of Sedna and 2000 CR_{105}?" The simplest requirement is that both Sedna and 2000 CR_{105} orbital parameters (semimajor axis, perihelion distance and orbital inclination) should be inside the distribution of the orbits created by the companion. However, even with such a small number of representatives of the IOC, some inference about the right shape of this population can be deduced.

(1) The a–q distribution at $a \sim 500$ AU (Sedna's semimajor axis) should show Sedna well inside or in the lower part of the q distribution for that a-band. This is statistically expected, since if Sedna is in the upper bound of the q distribution, then other objects with lower q should have been discovered by now.

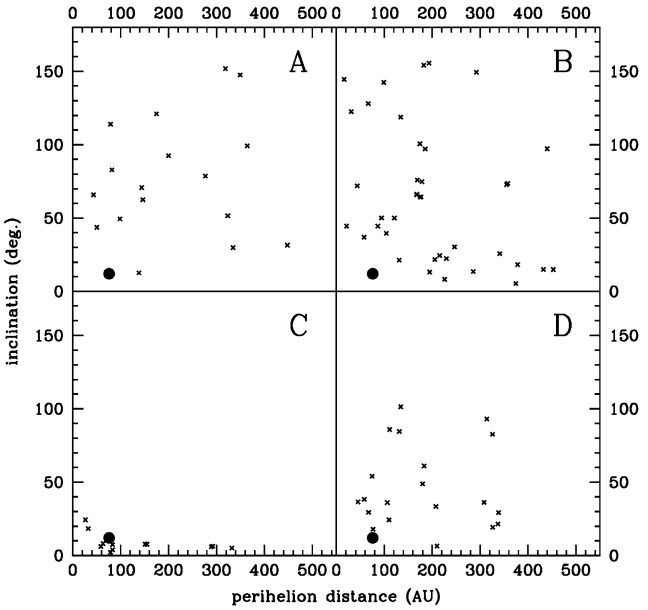

Fig. 13. Distributions of perihelia and inclinations for semimajor axes between 450 and 550 AU, coming from the eccentric companions integrations of Section 3.1 (panels A to C, respectively for $a_c = 5000$ AU, $a_c = 1500$ AU and $a_c = 1000$ AU) and from the migration integration of Section 3.2 (panel D). The integration times for panels A to D are, respectively, 1 billion years, 2 billion years, 2 billion years and 4.5 billion years and results correspond to Figs. 6, 8, 7 and 9, respectively. The large circle stands for Sedna's orbit.

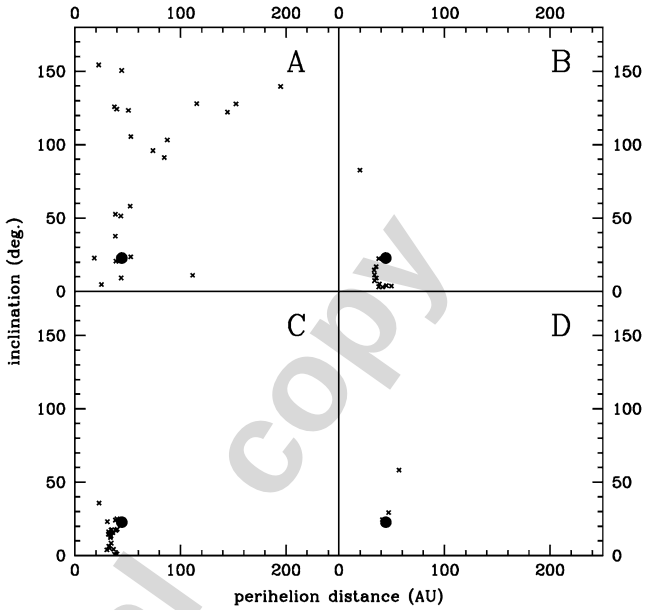

Fig. 14. Distributions of perihelia and inclinations for semimajor axes between 190 and 220 AU, coming from the eccentric companions integrations of Section 3.1 (panels A to C, respectively for $a_c = 5000$ AU, $a_c = 1500$ AU and $a_c = 1000$ AU) and from the migration integration of Section 3.2 (panel D). The integration times for panels A to D are, respectively, 1 billion years, 2 billion years, 2 billion years and 4.5 billion years and results correspond to Figs. 6, 8, 7 and 9, respectively. The large circle stands for 2000 CR_{105} orbit.

(2) The condition (1) should be more or less satisfied also by 2000 CR_{105} orbit, but here we do not need to be so strict since there are two other TNO's (2002 GB_{32} and 2001 FP_{185}) with a around 220 AU but lower q. In this sense, 2000 CR_{105} could well be in the upper part of the a–q distribution around 220 AU.

(3) Sedna should also stay near the inner edge of the a–q distribution for a q as high as Sedna's. So one should not expect a population with many objects with $q \sim 76$ AU and $a \sim 200$ AU or less. These would be expected to be spotted before Sedna, as they spend a larger fraction of the time at more easily observable distances.

(4) The distribution of inclinations around Sedna must contain small inclination members. We cannot be too conclusive about the inclination distribution of the DDO's based on a single representative. Nevertheless, the discovery of Sedna at a low orbital inclination from an all-sky survey (Brown et al., 2004) strengthens the point that Sedna is likely to belong to a small inclination population.

To better identify Sedna's and 2000 CR_{105} orbits inside the distributions induced by eccentric companions, we focus our attention at the semimajor axis bands around either object. Fig. 13 refers to semimajor axes from 450 to 550 AU (Sedna case) whereas Fig. 14 refers to semimajor axes from 190 to 250 AU (2000 CR_{105} case). In each panel we plot the distribution of perihelia and inclinations. Panels A to C refer, respectively, to the eccentric cases (no migration) for semimajor axis 5000, 1500 and 1000 AU as described in Section 3.1. Panel D refers to the migration case. In both figures, the observed object (Sedna or 2000 CR_{105}) is plotted as a big circle. Integration times in panels A to D are, respectively, 1 billion, 2 billion, 2 billion and 4.5 billion years. Now we try to answer the question at the top of this section using these figures and also Figs. 6–8. When comparing panels A to D, take into consideration also that perihelion distributions tend to shift towards higher values as times lapses.

The q–i distribution for the large companion (Figs. 13 and 14, panel A) may be compatible with point 4 above, although we might better expect some lower q and i for the Sedna case. The argument against this large companion is certainly point (3) above (Fig. 6). One must have in mind that this feature will be even enhanced if the integration is taken to Solar System age. So the probability of finding an object with Sedna's perihelion distance but smaller semimajor axis would be much higher than that of finding Sedna itself. This large companion model has however the advantage of producing the observed tilt of the invariable plane of the known planets relative to the Sun's equator at Solar System age (see Section 4.1).

The companions represented by panels B and D in Figs. 13 and 14 have the same orbital parameters except for the inclinations, $i_c = 40°$ in the case of the migration model (Fig. 9) and $i_c = 90°$ for the static case in Fig. 8. The q–i distributions for both cases look nice, with perhaps more advantage for the 90° case, although this should not be a decisive factor. Points 1 and 2 above are also nicely satisfied and so is point 4, although a somewhat smaller ρ_c might do a better job in this case, but anyway Sedna does not need to be in the very left edge of the a–q distribution since some randomness and the finding of larger objects also influence first discoveries.

The Earth mass planet model (panel C in Figs. 13 and 14 and Fig. 7) also satisfies points 1 to 3 fairly well. Point (4) is especially nicely satisfied. Note that although 2000 CR_{105} is in the upper part of the q distribution for its semimajor axis but this is not really incompatible with discovering 2000 CR_{105}. Also one must consider that at Solar System age the distribution will tend towards higher perihelia. Another feature of this Earth mass planet is that it seems to induce a greater amount of DDO's, by the mechanism in Gomes et al. (2005a) of which 2004 XR_{190} seems to be a member.

Gomes et al. (2005a) show that it is possible just by the perturbation of the known planets to reproduce 2000 CR_{105} orbits. This is done by the interplay of mean motion and Kozai resonances with Neptune. Nevertheless many more objects with 2000 CR_{105} perihelion distance and smaller semimajor axis should have been already discovered by statistical inference from Gomes et al. (2005a) model. Now the companion model can also make more objects available near 200 AU at Solar System age coming from the IOC reservoir induced by the companion. These objects can have their perihelia raised by the Gomes et al. (2005a) mechanism. In fact, from the four objects close to 2000 CR_{105} in (a, q) (Fig. 9), two of them came from the IOC.

In summary, considering all points above, it is a fair conclusion that the companion model is quite robust in producing nice DDO's and IOC's that include both Sedna and 2000 CR_{105} orbits and are also compatible with their early discoveries.

4. Other implications of a solar companion

We discuss here interactions of the hypothetical companion with the known planets and the observable Oort comet cloud.

4.1. Secularly precessing the "invariable" plane

We can reinterpret the last term in Eq. (2) to determine the orbit normal precession of the invariable plane due to the companion. Treating the known planets as aligned circular orbits, we construct the total angular momentum of the planets

$$\mathbf{L} = \sum_p M_p \sqrt{\mathrm{G}M_\odot r_p}\,\hat{\mathbf{n}}_p, \tag{11}$$

from which we obtain

$$\langle \dot{\mathbf{L}} \rangle = \boldsymbol{\Omega}_\mathbf{c} \times \mathbf{L}, \tag{12}$$

where

$$\boldsymbol{\Omega}_\mathbf{c} \equiv -\frac{3\sqrt{\mu_\odot}\rho_c \cos i_c}{4M_\odot} \frac{\sum_p M_p r_p^2}{\sum_p M_p \sqrt{r_p}} \hat{\mathbf{n}}_c. \tag{13}$$

In the Solar System lifetime, the invariable plane normal would be deflected through an angle $t_{ss}\Omega_c \sin i_c$, which equals the observed angle between the normal to the present planetary invariable plane and the Sun's rotation axis of 6° when

$$\rho_c |\sin 2i_c| \approx 3 \times 10^{-13}\ \mathrm{M}_\odot\,\mathrm{AU}^{-3}. \tag{14}$$

This requires a companion perturbation strength that is a factor of about 40 times as large as the minimum required to detach Sedna. If a companion has been responsible for the precession, its orbit normal, $\hat{\mathbf{n}}_c$, must lie in a plane with a normal direction parallel to $\Delta\mathbf{L}$. These analytic results have been confirmed in the numerical simulation with the 5 M_J companion presented in Section 3.1; this companion's orbital parameters satisfy the condition given in Eq. (14).

4.2. Perturbations of observable Oort cloud comets

Matese et al. (1999) (see also Matese and Lissauer, 2002) have argued that there is evidence of an impulsive component in the observed flux of OOC comets. The evidence consists of an overpopulated band of major axis orientations which also have an anomalous distribution of cometary orbital parameters consistent with a weak impulsive perturbation assisting the dominant galactic tidal interaction. No such anomaly was found in the observed IOC comet population. A summary of their analysis follows, beginning with the evidence that the galactic tidal perturbation dominates in making OOC comets discernable.

Saturn and Jupiter provide an effective dynamical barrier to the migration of OOC comet perihelia. OOC comets that are approaching the planetary zone at the present time were unlikely to have had a prior perihelion, q_{prior}, that was interior to the "loss cylinder" radius, $q_{\mathrm{lc}} \approx 15$ AU, when it left the planetary region on the present orbit. The simplifying assumption $q_{\mathrm{lc}} < q_{\mathrm{prior}}$ is then made for the present orbit. During the present orbit comet perihelion will then have been changed by the galactic tide (and by any impulsive perturbations from the hypothetical companion or passing stars). The orbital elements just before re-entering the planetary region on the present orbit are commonly referred to as "original" and will be, in essence, the observed values with the exception of a (perturbations by the major planets do not significantly change any other orbital element of OOC comets). Thus q_{prior} is changed to $q_{\mathrm{original}} \approx q_{\mathrm{obs}}$ during the course of the present orbit. As an observed comet ($q_{\mathrm{obs}} < q_{\mathrm{discernable}}$) leaves the planetary region again, the semimajor axis will have been changed from a_{original} to a_{future}, i.e., $a_{\mathrm{future}} \equiv a_{\mathrm{prior}}$ for the *next* orbit (neglecting stellar perturbations). In this context, Fig. 12 shows a sampling of "osculating" elements and cannot be compared directly with cataloged "original" or "future" data for observed comets. The Comet Catalogue indicates that ≈11% of original OOC comets exit the planetary region as future OOC comets, i.e., the discerned population of OOC comets should be dominated by first time entrants to the loss cylinder.

For near-parabolic comets, the angular momentum per unit mass determines the perihelion distance, $\mathbf{H} \equiv \sqrt{\mu a}\,\mathbf{h} \approx \sqrt{2\mu q}\,\hat{\mathbf{h}}$. With these assumptions, an OOC comet discernable for the first time had perihelion distances $q_{\mathrm{obs}} \leqslant q_{\mathrm{discernable}} < q_{\mathrm{lc}} \leqslant q_{\mathrm{prior}}$. Therefore, reducing q in a single orbit requires a decrease in angular momentum from the galactic tidal torque (and/or from an angular momentum impulse by the hypothetical companion or stars),

$$\Delta\mathbf{H} \equiv \mathbf{H}_{\mathrm{obs}} - \mathbf{H}_{\mathrm{prior}}, \quad \text{or}$$
$$q_{\mathrm{obs}} = q_{\mathrm{prior}} + \left(2\Delta\mathbf{H}\cdot\mathbf{H}_{\mathrm{obs}} - \Delta\mathbf{H}^2\right)/2\mu. \tag{15}$$

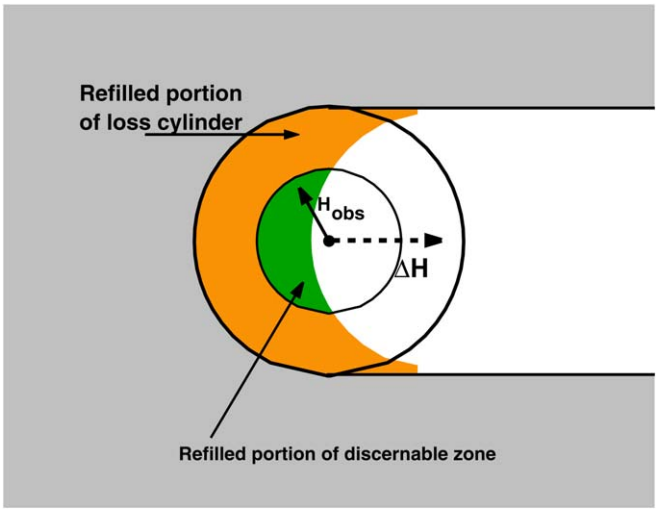

Fig. 15. The mapping model showing the displacement, $\Delta\mathbf{H}$, of the specific angular momentum phase space, $\mathbf{H}$, for a specified semimajor axis and major axis orientation (pointed out of the page) in the course of a single orbit. The *prior* filled distribution (light gray region) is outside the loss cylinder boundary (large circle of radius $\sqrt{2\mu q_{\rm lc}}$). All prior phase space points, filled and empty, are uniformly displaced by the perturbation ($\Delta\mathbf{H} = \mathbf{H}_{\rm obs} - \mathbf{H}_{\rm prior}$). If $\Delta\mathbf{H}$ moves the prior loss cylinder boundary inside or beyond the discernable zone (small circle of radius $\sqrt{2\mu q_{\rm discernable}}$), perturbations can make comets discernable (green region) for this major axis orientation and semimajor axis. The arrow labeled $\mathbf{H}_{\rm obs}$ illustrates a specific phase space point that has been observed. Note in this illustration of a weak, purely tidal perturbation, all observed comets would have $S \equiv {\rm Sign}(\Delta\mathbf{H}_{\rm tide} \cdot \mathbf{H}_{\rm obs}) = -1$.

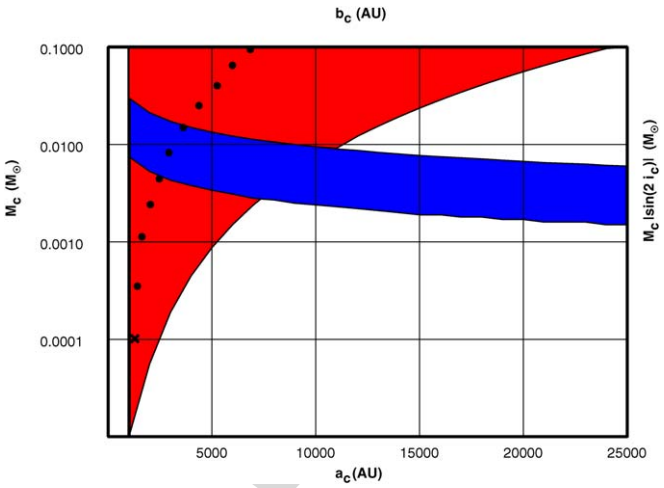

Fig. 16. The companion mass-distance relations: (red) the region $M_c > 0.8 \times 10^{-14}\ {\rm M}_\odot\ {\rm AU}^{-3}\ b_c^3$ describing the requirements to detach Sedna. (Dots) The curve $M_c|\sin(2i_c)| = 3 \times 10^{-13}\ {\rm M}_\odot\ {\rm AU}^{-3}\ b_c^3$ describing the requirements to precess the invariable plane by 6°. (Cross) The companion parameters used in the migration model of Figs. 9–12. (Blue) The range of values $M_c \approx {\rm M}_\odot\ {\rm AU}^{1/2}/\sqrt{4a_c}$ required to explain the outer Oort cloud comet anomaly.

A perturbation that completely refills the discernable region would have (see Fig. 15)

$$|\Delta\mathbf{H}| > \sqrt{2\mu q_{\rm lc}} + \sqrt{2\mu q_{\rm discernable}}, \tag{16}$$

while the weakest perturbation that could make a comet discernable would reduce the prior perihelion distance from $q_{\rm prior} \approx q_{\rm lc}$ to $q_{\rm obs} \approx q_{\rm discernable}$, i.e.,

$$|\Delta\mathbf{H}|_{\rm min} = \sqrt{2\mu q_{\rm lc}} - \sqrt{2\mu q_{\rm discernable}}. \tag{17}$$

The galactic disk tidal perturbation predicts the secular change

$$|\Delta\mathbf{H}| \propto a^{7/2}\big|\sin(2B)\big|, \tag{18}$$

where B is the galactic latitude of the major axis and the semimajor axis is the original value.

Observational evidence that is commonly referred to indicating that the galactic tide dominates in making OOC comets discernable is embodied in this equation. The observed galactic latitude distribution is deficient near $B = 0°$, 90° and 180° because fewer comets have values of a with $|\Delta\mathbf{H}| > |\Delta\mathbf{H}|_{\rm min}$ for these values.

More subtle evidence of the tidal imprint is discussed in Matese and Lissauer (2004), in which Eq. (15) plays the major role. We see there that if the statistic

$$S \equiv {\rm Sign}(\Delta\mathbf{H}_{\rm tide} \cdot \mathbf{H}_{\rm obs}) \tag{19}$$

is equal to -1, then the comet perihelion more nearly has "just entered" the discernable zone, while $S = +1$ indicates that the comet perihelion more nearly is about to leave it. Now for large-a OOC comets, the tidal perturbation is sufficiently large that the discernable zone is nearly completely refilled so that $S = \pm 1$ should be almost equally likely. In Matese and Lissauer (2004) this is found to be so for 33,000 AU $< a$. In contrast, for $a <$ 33,000 AU a statistically significant preponderance of $S = -1$ is found, in agreement with the notion that the $a^{7/2}$ dependence of $\Delta\mathbf{H}_{\rm tide}$ rapidly decreases in strength as a decreases. In this simple modeling then, comets with 33,000 AU $< a$ completely fill the discernable region due to the tide alone, those with 25,000 AU $< a <$ 33,000 AU only partially refill the discernable region due to the tide alone and $a <$ 25,000 AU comets would not refill any of the discernable region since $|\Delta\mathbf{H}_{\rm tide}| < |\Delta\mathbf{H}_{\rm min}|$.

How then would an weak impulsive perturbation be expected to manifest itself observationally in this simple model? For 33,000 AU $< a$, comets would completely refill the discernable zone due to the tide, and an impulse will largely not add to the number of comets observed, it will only change the identity of the comets made discernable. In contrast, Fig. 15 suggests that for 25,000 AU $< a <$ 33,000 AU, an angular momentum impulse that constructively adds to $\Delta\mathbf{H}_{\rm tide}$ can make the discernable region refill more nearly completely. In addition, $a <$ 25,000 AU comets that would not be discernable in the presence of the tide alone can now partially refill the discernable region if the impulse aids the tide. Therefore, the signature of a weak impulsive perturbation to OOC comets would be an enhanced number of observed near-parabolic OOC comets with major axes near the orbital plane of the impulsive perturber. The excess of comets would preferentially have $a <$ 33,000 AU and therefore a larger proportion of $S = -1$ than in the non-perturbed population. The angular extent of the overpopulated band would suggest whether it was produced by a passing star or a bound solar companion.

An enhanced band of angular half-width $\beta \approx 0.2$ radians has been reported (Matese et al., 1999; Matese and Lissauer, 2004). The distributions of a and S within the band are consistent with the population being impulsively enhanced for $a < 33{,}000$ AU, as just discussed. The arc of the band is too long to be associated with a stellar impulse, therefore a bound perturber has been hypothesized. They infer the parameters of the object by assuming that $|\Delta\mathbf{H}|_{\text{impulse}} \approx |\Delta\mathbf{H}|_{\min}$. In contrast, any IOC comets similarly impulsed by the perturber would be largely unaffected by the galactic tide and would not be made observable since the impulse alone is too weak. Any hypothetical companion presently in the IOC region may have largely cleared out the IOC cometary phase space accessible to its impulses during the Solar System lifetime. Conversely, galactic tides and weak stellar impulses tend to randomize the OOC cometary phase space over timescales that are short compared to the depletion timescale due to the hypothetical companion.

The impulse approximation is (Matese et al., 1999)

$$|\Delta\mathbf{H}|_{\text{impulse}} \approx |\mathbf{r} \times \mathbf{\Delta v}| \approx \frac{2GM_c\sqrt{2/3}}{U\beta}, \tag{20}$$

where the relative velocity of the near-parabolic comet orbit and the elliptical companion orbit is $U \approx \sqrt{2\mu/r_c}$. Equating $|\Delta\mathbf{H}|_{\text{impulse}}$ to $|\Delta\mathbf{H}|_{\min}$ and further setting $r_c \approx a_c$ and $q_{\text{discernable}} \approx 5$ AU, we obtain

$$M_c \approx \mathrm{M}_\odot\,\mathrm{AU}^{1/2}/\sqrt{4a_c}. \tag{21}$$

The orbit normal direction of a companion consistent with this anomaly would be perpendicular to the plane centrally located within the band.

In Fig. 16 we illustrate (i) the region of M_c versus b_c that would detach Sedna [Eq. (8)], (ii) the curve $M_c|\sin(2i_c)|$ versus b_c for precessing the invariable plane by 6° [Eq. (14)], and (iii) the band of values, including the estimated uncertainties, for creating the outer Oort cloud comet anomaly [Eq. (21)]. Fig. 16 indicates that there is a companion mass/distance consistent with all three effects. However, an analysis indicates that the orbit normal, $\hat{\mathbf{n}}_c$, which is consistent with the Oort cloud anomaly is oriented ≈65° from the direction $\Delta\mathbf{L}$, the deflection of the invariable plane angular momentum. This is sufficiently different from the required 90° that we would conclude that a companion with the parameters required to create the Oort cloud anomaly at the present epoch is unlikely to be able to precess the invariable plane over 4.5×10^9 years. But a companion mass of 3–10 $\mathrm{M_J}$ at distances of 5000–10,000 AU is consistent with the observable Oort comet cloud anomaly and with that capable of producing Sedna and the DDP.

5. Summary and conclusions

We have demonstrated that a distant planetary-mass solar companion (i.e., a planet orbiting within the inner Oort cloud) would be capable of raising the perihelia of scattered disk objects and placing them on orbits similar to those of Sedna and 2000 $\mathrm{CR_{105}}$. The perihelia of the SDO's are raised by the Kozai mechanism, so the orbit of such a hypothetical companion would in principle need to be substantially inclined to that of the orbit of the scattered disk object that was produced by perturbations of the known planets in order for the type of perturbations that we are discussing to operate efficiently. Note, however, that a very eccentric Earth mass companion with small perihelion (60 AU in the example that we studied) and low inclination could also produce low inclination Sedna-like orbits. The required minimum companion mass would be only about Neptune's mass if it orbited with semiminor axis at 2000 AU, but would need to be a Jupiter mass at 5000 AU and 8 Jupiter masses at 10,000 AU. A 1 $\mathrm{M_\oplus}$ planet with, e.g., $a_c = 1000$ AU, $e_c = 0.94$ (thus $b_c = 341$ AU) and $i_c = 5°$ would also be capable of providing the requisite perturbations.

Our solar companion model presents a viable alternative to the stellar encounter scenarios proposed and analyzed by Morbidelli and Levison (2004). One major difference between the models is that the solar companion could produce a 'live' inner Oort cloud population, whereas stellar encounter models create a fossil population. This may have important consequences on the influx of comets into the inner Solar System. Note that both models place the two observed DDO's near the edge of the produced distribution, but any modeling effort which tries to minimize the demands on a hypothesized perturber necessarily places at least one of the observed objects close to the edge of the theoretical distribution.

A significant advantage of the solar companion model is that it naturally produces the very massive inner Oort cloud that is suggested by observations to date. The passing star perturber model creates only around 0.1 $\mathrm{M_\oplus}$. A brown dwarf's planetesimals captured by the Sun can amount to a large mass, but the inclination distribution could favor any arbitrary initial plane (including retrograde). While there is some preference for discovery of low vs high inclination objects, Sedna's low inclination would need to be regarded as coincidentally low.

A Neptune-mass companion at 1500 AU would have a visual magnitude of ≈25 and may be marginally observable in Pan STARRS (2006). Its intrinsic IR luminosity has not been modeled as yet. Matese et al. (2006) conclude that a Jupiter mass companion capable of producing the DDP would have been seen in the 12 μm IRAS band while an 8 $\mathrm{M_J}$ companion capable of producing the DDP could have been recorded in the 1.2 μm (J-band) 2MASS database. It is noted that even if it has been recorded in these databases, it is unlikely that it would have been *recognized* as a Jupiter mass companion and cannot be rejected on that basis. An eccentric companion could be fairly bright at perihelion but most of the time it would be too faint to be visible by present observational capabilities. As an example, considering the Earth-mass companion, with a density of 1.2 $\mathrm{g/cm^2}$ and an albedo of 0.5, the companion would have a magnitude greater than 24, 85% of the time.

A small mass companion (roughly Earth to Neptune mass) could have formed within the planetary region, been ejected to its current heliocentric distance by gravitational scatterings of Jupiter and Saturn. Such a body may have been ejected from the Solar System after producing the DDP, or it could remain as the largest member of the standard scattered disk population. Or its perihelion could have been raised by perturbations of passing stars which would have needed to have been passing at a closer

distance than would be reasonable to hypothesize subsequent to the dispersal of the Sun's birth cloud/cluster, but not as close as required for direct stellar perturbations producing the observed high perihelion scattered disk objects. A Jupiter mass or larger object on a highly inclined orbit beyond 5000 AU would most likely have formed as a small, distant binary-star like companion, e.g., by fragmentation during collapse or capture.

Acknowledgments

R.S.G. received support from Conselho Nacional de Desenvolvimento Científico e Tecnológico. J.J.L. received support from NASA Planetary Geology and Geophysics Grant 344-30-50-01.

References

Brown, M.E., Trujillo, C., Rabinowicz, D., 2004. Discovery of a candidate inner Oort cloud planetoid. Astrophys. J. 617, 645–649.

Chambers, J.E., 1999. A hybrid symplectic integrator that permits close encounters between massive bodies. Mon. Not. R. Astron. Soc. 304, 793–799.

Dones, L., Levison, H.F., Duncan, M.J., Weissman, P.R., 2005. Simulations of the formation of the Oort cloud I. Preprint.

Duncan, M.J., Levison, H.F., Dones, L., 2004. Dynamical evolution of ecliptic comets. In: Festou, M.C., Keller, H.U., Weaver, H.A. (Eds.), Comets II. Univ. of Arizona Press, Tucson, pp. 193–204.

Emel'yanenko, V.V., Asher, D.J., Bailey, M.E., 2003. A new class of trans-neptunian objects in high-eccentricity orbits. Mon. Not. R. Astron. Soc. 338, 443–451.

Fernández, J.A., Brunini, A., 2000. The buildup of a tightly bound comet cloud around an early Sun immersed in a dense galactic environment: Numerical simulations. Icarus 145, 580–590.

Goldreich, P., 1965. Inclination of satellite orbits about an oblate precessing planet. Astron. J. 70, 5–9.

Gomes, R.S., Gallardo, T., Fernández, J.A., Brunini, A., 2005a. On the origin of the high-perihelion scattered disk: The role of the Kozai mechanism and mean motion resonances. Celest. Mech. Dyn. Astron. 91, 109–129.

Gomes, R.S., Levison, H.F., Tsiganis, K., Morbidelli, A., 2005b. Origin of the cataclysmic Late Heavy Bombardment period of the terrestrial planets. Nature 435, 466–469.

Matese, J.J., Lissauer, J.J., 2002. Continuing evidence of an impulsive component of Oort cloud cometary flux. ESA SP-500 (2002) 309–314.

Matese, J.J., Lissauer, J.J., 2004. Perihelion evolution implies the dominance of the galactic tide in making Oort cloud comets discernable. Icarus 170, 508–513.

Matese, J.J., Whitman, P.G., Whitmire, D.P., 1999. Cometary evidence of a massive body in the outer Oort cloud. Icarus 141, 354–366.

Matese, J.J., Whitmire, D.P., Lissauer, J.J., 2006. A wide-binary solar companion as a possible origin of Sedna-like objects. Earth Moon Planets. Special edition of ACM2005. In press.

Morbidelli, A., Levison, H., 2004. Scenarios for the origin of the orbits of the trans-neptunian objects 2000 CR_{105} and 2003 VB_{12}. Astron. J. 128, 2564–2576.

Morbidelli, A., Levison, H.F., Tsiganis, K., Gomes, R.S., 2005. Chaotic capture of Jupiter's trojan asteroids in the early Solar System. Nature 435, 462–465.

Pan STARRS, 2006. http://pan-starrs.ifa.hawaii.edu/public/science/stars.html.

Tsiganis, K., Gomes, R.S., Morbidelli, A., Levison, H.F., 2005. Origin of the orbital architecture of the giant planets of the Solar System. Nature 435, 459–461.

Wolfram Research, 2003. Mathematica 5.